

Nanoscale

Accepted Manuscript



This is an *Accepted Manuscript*, which has been through the Royal Society of Chemistry peer review process and has been accepted for publication.

Accepted Manuscripts are published online shortly after acceptance, before technical editing, formatting and proof reading. Using this free service, authors can make their results available to the community, in citable form, before we publish the edited article. We will replace this *Accepted Manuscript* with the edited and formatted *Advance Article* as soon as it is available.

You can find more information about *Accepted Manuscripts* in the [Information for Authors](#).

Please note that technical editing may introduce minor changes to the text and/or graphics, which may alter content. The journal's standard [Terms & Conditions](#) and the [Ethical guidelines](#) still apply. In no event shall the Royal Society of Chemistry be held responsible for any errors or omissions in this *Accepted Manuscript* or any consequences arising from the use of any information it contains.

Cite this: DOI: 10.1039/c0xx00000x

www.rsc.org/xxxxxx

ARTICLE TYPE

A Redox-Responsive Mesoporous Silica Nanoparticle Capped with Amphiphilic Peptides by Self-assembly for Cancer Targeting Drug Delivery

Dong Xiao, Hui-Zhen Jia, Ning Ma, Ren-Xi Zhuo, and Xian-Zheng Zhang*

Received (in XXX, XXX) Xth XXXXXXXXX 20XX, Accepted Xth XXXXXXXXX 20XX

DOI: 10.1039/b000000x

A redox-responsive mesoporous silica nanoparticle (RRMSN) was developed as a drug nanocarrier by noncovalent functionalization of MSNs with amphiphilic peptides containing RGD ligand. The alkyl chain stearic acid (C₁₈) with thiol terminal group was anchored on the surface of MSNs *via* disulfide bond, and the amphiphilic peptide (AP) C₁₈-DSDSDSDSRGDS was coated by self-assembly through hydrophobic interactions between the octadecyl groups of MSNs and alkyl chains of AP, which played the role of gatekeeper collectively. *In vitro* drug release profiles demonstrated that anticancer drug (DOX) could be entrapped with nearly no leakage in absence of dithiothreitol (DTT) or glutathione (GSH). With addition of DTT or GSH, the entrapped drug released quickly due to the cleavage of disulfide bond. It was found that after the internalization of MSNs by cancer cells *via* the receptor-mediated endocytosis, the surface amphiphilic peptides and alkyl chain of RRMSN/DOX were removed to induce rapid drug release intracellularly after the cleavage of disulfide bond, triggered by GSH secreted in cancer cells. This novel intelligent RRMSN/DOX drug delivery system by using self-assembly of amphiphilic peptides around the MSNs provides a facile, but effective strategy for the design and development of smart drug delivery for cancer therapy.

Introduction

Nowadays, cancer is regarded as one of the most common causes of human death, and chemotherapy, which remains to be one of the most frequently used cancer treatments, often causes systemic side effects due to toxicity by the nonspecific distribution of anti-cancer drugs.¹⁻⁴ In the past two decades, nanotechnology has brought out a far-reaching influence on cancer therapy.^{5,6} Since traditional drugs have no ability to distinguish between cancerous and normal cells, a variety of nanoscale drug delivery systems, such as polymer conjugates, dendrimers, cyclodextrin, micells, liposomes and inorganic nanoparticles, have been developed to capitalize on enhanced permeability and retention (EPR) effect and endorse site-specific delivery.⁷⁻⁹ Among the proposed drug delivery systems (DDSs), mesoporous silica nanoparticles (MSNs) have been turned out to be superior hosts for molecules of diverse sizes, shapes, and functionalities. Owing to the distinctive mesoporous structure, large surface area, tunable pore size, good biocompatibility, and well-defined surface properties, MSNs have been intensively suggested for use in controlled drug/gene release, biosensors, bio-markers, enzyme supporters.¹⁰⁻¹⁴ MSNs can be end-capped with multitudinous gatekeepers, such as nanoparticles, supramolecular nanovalves, polymers, biomolecules, peptides, which can be maneuvered by triggering motifs, including redox,^{15,16} pH,¹⁷ temperature,¹⁸ photo,¹⁹ electrostatics,²⁰ enzymatic activity,²¹ magnetic actuation.²² For example, Cai's group reported the fabrication of nanoreservoirs

based on MSNs that are end-capped with collagen and demonstrated great potential for both cell-specific targeting and redox-responsive controlled drug release.¹² Zhu and co-workers designed a temperature-dependent controlled release system based on poly(N-isopropylacrylamide) (PNiPAm)-functionalized mesoporous silica materials.²³ Kim and co-workers designed a novel cyclodextrin(CD)-covered nanocontainer system that contained a photocleavable linker and could exhibit photo-responsive release characteristics.²⁴ Perez-Paya and co-workers described the use of a simple tripeptide containing a Fmoc protecting group that allowed the gate to be colsed by π - π interactions between adjacent Fmoc moieties.²⁵ Heise's group reported a novel enzyme-mediated release mechanism that takes advantage of well understood, and chemically straightforward Fmoc chemistry to generate specific gatekeepers from a selection of the 20 natural amino acids.²⁶

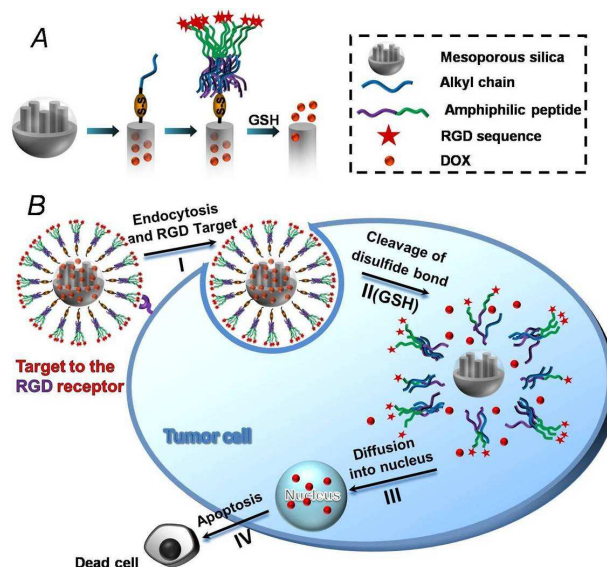
As we know, peptides have been widely used for controlled drug delivery due to their inherent bioactivity, biodegradability and well biocompatibility.²⁷ Due to the specific bioactivity of peptides, peptide-based DDSs could achieve improved drug fraction of bioavailability, enhanced drug targeting property, increased biocompatibility and reduced side-effect.^{28,29} In particular, short peptide chains have attracted a great deal of attention in recent years on account of their tunable functionality, biodegradability, and relative ease of synthesis.^{30,31} It has been well-known that RGD and IL-13 can be used for targeting nanoparticles to specific cancer cell lines.³²⁻³⁴ Moreover, some peptide sequences (e.g. TAT peptide) demonstrated cell

penetrating and endosomal escape properties.^{35,36} Of the most peptides, amphiphilic peptides are increasingly appealing as molecular building blocks in the bottom-up fabrication of supramolecular structures based on self-assembly and have potential in a multitude of significant applications in the fields of biotechnology and bioengineering. Peptide-based amphiphiles as molecular building blocks are constituted of four main categories, in which hydrophilic amino acid sequences coupled to hydrophobic alkyl chains at either the *N*- or the *C*-terminus have been intensely exploited recently.³⁷ Conventionally, peptides are covalently attached to the silica surface through additional cross-linking reagents and intractable synthetic methods once in a while, which results in poor surface grafting density. For the sake of getting over the problems, investigators developed a straightforward method to functionalize MSNs with short peptide chains by using self-assembly of amphiphilic peptides around the hydrophobic MSNs. In this way, amphiphilic peptides were noncovalently modified onto the alkyl chains, leading to a high surface grafting density, which may come into a dense reticular or membrane structure. As a result, the pores of MSNs were capped by hydrophobic interactions between the alkyl chains, realizing “zero release”.³⁸

Since traditional antineoplastic drugs cannot discern between diseased and normal cells, most researchers have focused on realizing selective drug release at cancerous tissues. Recently, apart from taking advantage of the enhanced permeation and retention (EPR) effect, to further improve the delivery efficiency, cancer specific recognition and accumulation of MSN-based nanocarrier in the cancer site, active targeting ligands, such as folate,³⁹ peptides (e.g., Arg-Gly-Asp (RGD)⁴⁰ or cell penetrating peptides⁴¹) and antibodies,⁴² have been conjugated to drug carriers, which have been proved to be able to recognize and bind to specific receptors/integrins overexpressed on the surface of cancer cells.^{43,44}

Of the most stimuli, redox-responsiveness is frequently investigated due to that the glutathione (GSH) concentration in different sites varies tremendously.^{45,46} GSH molecules are located in the cellular cytoplasm with a concentration of 2-10 mM, secreted by cancer cells, which is much higher than that in blood (ca. 2 μ M).⁴⁷ Taking into account of above considerations, here we report on a facile, but effective self-assembly method to design a redox-responsive drug delivery system based on RGD containing amphiphilic peptide-capped MSNs, named RRMSN/DOX. As shown in Scheme 1A, MSNs were modified with a stearic acid (Cys-C₁₈) *via* disulfide linkages, and amphiphilic peptide (AP) containing RGD sequence (C₁₈-DSDSDSDSRGDS) was attached to the octadecyl modified MSN surfaces in aqueous media through hydrophobic interactions between octadecyl groups of MSNs and alkyl chains of AP.³⁶ The anticancer drug, doxorubicin (DOX), was loaded in the cores of RRMSN. The amphiphilic peptide and the stearic acid synergistically served as gatekeeper to allow the gate to be closed by hydrophobic interactions between alkyl chains or the dense reticular or membrane structure by self-assembly of AP. As illustrated in Scheme 1B, once the MSNs were accumulated in cancer cells *via* the receptor-mediated endocytosis, the surface APs and alkyl chains of RRMSN/DOX were removed to induced rapid drug release intracellularly after the cleavage of disulfide

bond, triggered by GSH secreted in cancer cells.^{45,47} The tunable release behavior of the entrapped drug in RRMSN/DOX with self-assembled AP gatekeeper was studied and the targeted drug delivery in cancer cells was also investigated.



Scheme 1 (A) Schematic structure of RRMSN/DOX and redox-responsive cancer targeting drug delivery. (B) (I) cell uptake through RGD-mediated interaction; (II) glutathione-triggered drug release *via* cleavage of disulfide bond; (III) drug diffusing into the cytoplasm and eventually to the nucleus; (IV) apoptosis of cancer cells.

Results and discussion

70 Chemical Characterizations of MSN

Typical mesoporous silica nanoparticle (MCM-41) was used as the drug carrier, synthesized according to literature⁴⁶ with an average diameter of ~125 nm as shown in the scanning electron microscopy (SEM) image in Fig. 1A. The structure of the obtained MSN was characterized by transmission electron microscopy (TEM) image (Fig. 1C), revealing that the MSN exhibited a well-defined porous structure with a hexagonal arrangement. The N₂ sorption isotherms of the MSNs further revealed a Brunauer Emmett Teller (BET) typical isotherm of a MCM-41 structure (Fig. S1), with a surface area of 1090.0 m²/g (Fig. S2) and a narrow Barrett-Joyner-Halenda (BJH) pore-size distribution (average pore diameter: 3.0 nm) (Fig. 1B). The hydrodynamic diameter of MSN detected by dynamic light scattering (DLS) was 166 nm (PDI=0.175) (Fig. S3A).

85 Chemical Characterizations of Peptides

The amphiphilic peptide (AP) C₁₈-DSDSDSDSRGDS, was synthesized manually using standard fluorenylmethoxycarbonyl (Fmoc) solid phase peptide synthesis (SPPS)⁴⁹ technique, and the molecular weight of the peptide confirmed by ESI-MS as shown in Fig. S4 was 1506.0 [M+H]⁺ and 753.1 [M+2H]²⁺. The alkyl chain with thiol group C₁₈-Cys and control peptide C₁₈-DSDSDSDSDSDS were synthesized and examined in an identical way as described above. The molecular weight was shown in Fig. S5 and Fig. S6, respectively.

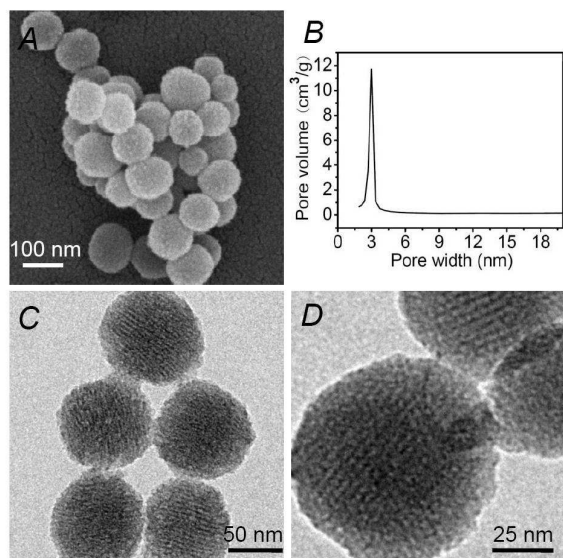


Fig. 1 (A) SEM image of MSNs; (B) BJH pore size distribution of MSNs; (C) TEM image of MSNs; (D) TEM image of MSN-S-S-C₁₈-Peptide/DOX (RRMSN/DOX).

5 Synthesis and Chemical Characterizations of MSN-S-S-C₁₈/DOX

As elucidated in Scheme 1A, for the preparation of mesoporous silica nanoparticles with peptide gatekeeper connected *via* disulfide linker, the surface of MSNs was initially functionalized with mercaptopropyl groups by treatment with 3-mercaptopropyl-trimethoxysilane to obtain MSN-SH containing thiol unit on the surface. Then, MSN-S-S-Pyridine, as active intermediate, was gained by reacting MSN-SH with 2-2'-dithiodipyridine at room temperature in the dark for 24 h. At the same time, DOX was efficiently loaded into the pore of silica particles by vigorous stirring the mixture of MSN-S-S-Pyridine nanoparticles and DOX solution for 24 h. Thenceforth, the alkyl chain with thiol group (C₁₈-Cys) was immobilized onto DOX loaded MSN-S-S-Pyridine *via* disulfide exchange to prepare MSN-S-S-C₁₈/DOX (Scheme S1). A thiol absorption band at 2560 cm⁻¹ was found in the FT-IR spectrum of MSN-SH (Fig. S7B), confirming the successful incorporation of the C₁₈-Cys. The thermal gravimetric analysis (TGA) curves shown in Fig. 2, also indicated the C₁₈-Cys was immobilized onto the MSN with success.

25 Synthesis and Chemical Characterizations of MSN-S-S-C₁₈-Peptide/DOX (RRMSN/DOX)

Amphiphilic peptides are particularly appealing as building blocks in the bottom-up fabrication of supramolecular structures based on self-assembly and have great potential, especially in biomedical materials, biotechnology and controlled drug delivery. Here, we demonstrated a simple and effective self-assembly approach to prepare a redox-responsive mesoporous silica nanoparticle (RRMSN) as drug delivery system. Amphiphilic peptide (AP) C₁₈-DSDSDSRSGDS was sonicated in deionized water, and MSN-S-S-C₁₈/DOX was slowly added to the system. The mixture were stirred at room temperature in the dark for 24 h. The resulting solid was centrifuged (8000 r/min, 10 min), washed thoroughly with DOX solution, water and methanol, and then dried under vacuum. Thereupon, the RRMSN/DOX was fabricated. The MCM-41 type of hexagonally packed mesoporous

structure of MSN was confirmed by transmission electron microscopy (TEM) (Fig. 1D). The hydrodynamic diameter of RRMSN/DOX was 180 nm (PDI = 0.273) (Fig. S3B) detected by dynamic light scattering (DLS). Noted here, the drug loading efficiency (DLE) of RRMSN/DOX was ~3.81 wt.% and the drug encapsulation efficiency (DEE) of RRMSN/DOX was ~8.86 wt.%, as determined by RF-5301PC spectrofluorophotometer (Fig. S8). The DLE was defined as follow: DLE = (mass of drug loaded in MSNs/mass of drug loaded MSNs) × 100%. The DEE was defined as follow: DEE = (mass of drug loaded in MSNs/mass of feed drug) × 100%. We also measured the DLE and DEE of RRMSN/DOX by ultraviolet (UV) absorbance using a ultraviolet standard calibration curve. The DLE and DEE were ~3.88 wt.% and ~8.94 wt.%, respectively, as determined. Also, the DLE of CRRMSN/DOX was determined by the identical way and the DLE of CRRMSN/DOX was ~3.84 wt.% as measured.

As indicated in the thermal gravimetric analysis (TGA) curves in Fig. 2, the weight loss of MSN-S-S-C₁₈-Peptide/DOX, MSN-S-S-C₁₈/DOX and MSN were 75.04%, 25.46% and 15.27%, respectively, when the temperature increased to 800 °C. The drug loading efficiency was approximately ~3.81 wt.%, thus, the weight loss of drug was negligible with respect to that of MSN-S-S-C₁₈/DOX. As a result, the increased weight loss of MSN-S-S-C₁₈/DOX further confirmed that the C₁₈-Cys was successfully conjugated into the nanoparticles. In addition, the weight loss of RRMSN/DOX (75.04%), in contrast with that of MSN-S-S-C₁₈/DOX (25.46%), indicated the noncovalent functionalization of MSNs with AP.

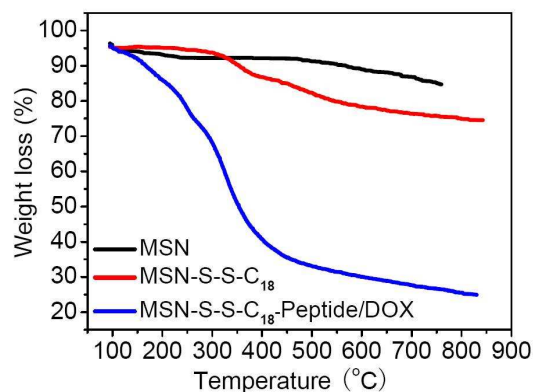


Fig. 2 TGA curves of different nanoparticles: MSN, MSN-S-S-C₁₈/DOX, MSN-S-S-C₁₈-Peptide/DOX (RRMSN/DOX).

In Vitro Release Profiles Studies

In order to understand the redox-responsive property of RRMSN/DOX with amphiphilic peptide gatekeepers *via* disulfide linkage, the drug release profiles with or without DTT and GSH were investigated. From Fig. 3A, there was nearly no DOX release during 4 h in the absence of DTT, making clear that DOX was efficiently confined in the pore reservoirs of RRMSN/DOX by capping of the amphiphilic shell. As shown in Fig. 3C, we could draw an identical research conclusion in absence of GSH. Our method was based on the spontaneous attachment of AP to the stearic alkyl modified MSN surfaces in aqueous media through hydrophobic interactions between stearic groups of MSNs and APs. The pores of the RRMSN/DOX were switched

off due to the hydrophobic interactions and the self-assembled structure of AP. In contrast, a burst release of DOX could be detected in existence of DTT or GSH due to the removal of peptide capping *via* the cleavage of disulfide bond, as reported in the literature.^{53,54} Further on, the release profiles at different DTT and GSH concentrations were researched. As shown in Fig. 3B and 3D, it was found that the DOX release rate increased with ever-increasing concentration of DTT or GSH,⁵⁵ which played a crucial role in the controlled drug delivery system, suggesting that the RRMSN/DOX have a potential to be an effective drug carrier and the noncovalently incorporated amphiphilic peptide can act as an effective nanovavle.

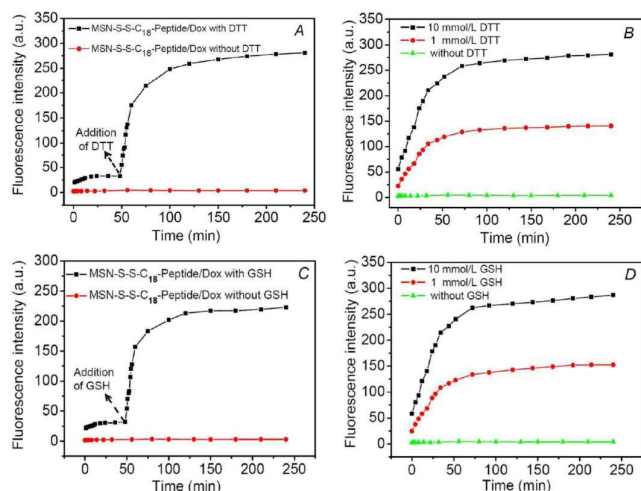


Fig. 3 Release profile of the loaded DOX from RRMSN/DOX. (A) Release profile of DOX at pH 7.4 with and without DTT; (B) DTT-responsive release profile of DOX at different DTT concentrations; (C) Release profile of DOX at pH 7.4 with and without GSH; (D) GSH-responsive release profile of DOX at different GSH concentrations.

Cellular Uptake Measured by CLSM

To investigate the cancer-targeting ability of RRMSN/DOX, MSN-S-S-C₁₈-Peptide/DOX nanoparticle was incubated with U-87 MG cells (human glioblastoma cell lines) and non-cancerous COS7 cells (African Green Monkey SV40-transf'd kidney fibroblast cell line) for 4 h and observed by using confocal laser scanning microscopy (CLSM). It was well-known that integrin $\alpha_v\beta_3$ was overexpressed in cancer cells and RGD motif could specifically bind cancer cells through RGD-integrin interactions.^{48,49} As shown in Fig. 4, a stronger red fluorescence was observed from U-87 MG cells incubated with RRMSN/DOX for 4 h than that from COS7 cells, indicating that more nanoparticles were taken up by cancer cells through RGD receptor-mediated target effect, which can recognize and bind to specific receptors/integrins overexpressed on the surface of cancer cells. As a result, the pore of RRMSN/DOX was switched on after the cleavage of disulfide bond in the presence of glutathione (GSH) secreted by cancer cells. The much stronger red fluorescence in U-87 MG cells confirmed the cancer cell targeting property.^{42,43}

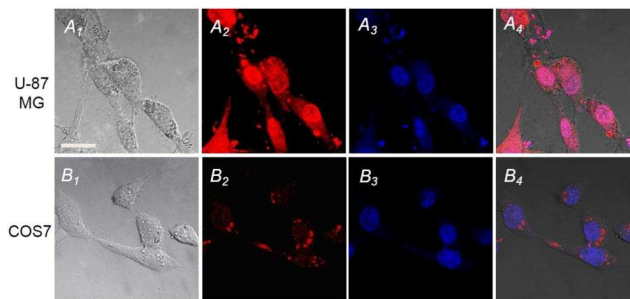


Fig. 4 Confocal laser scanning microscopy (CLSM) images of U-87 MG cells and COS7 cells treated by RRMSN/DOX for 4 h. A₁₋₄) U-87 MG cells co-incubated with RRMSN/DOX; B₁₋₄) COS7 cells co-incubated with RRMSN/DOX. Image 1: bright field; image 2: red fluorescence field; image 3: blue fluorescence field; image 4: overlapped field. Scale bar: 20 μm.

To further study the RGD receptor-mediated target, the no RGD sequence containing MSN-S-S-C₁₈-Peptide/DOX nanoparticle, as control group (CRRMSN/DOX), was synthesized. The RRMSN/DOX and CRRMSN/DOX nanoparticles were incubated with U-87 MG cells for 4 h. From Fig. 5A, apparent difference in red fluorescence was found. The stronger red fluorescence of RRMSN/DOX in U-87 MG cells than that of CRRMSN/DOX suggested that the targeting ability was attributed to the RGD sequence in amphiphilic peptide. As control, the RRMSN/DOX and CRRMSN/DOX nanoparticles were incubated with noncancerous COS7 cells for 4 h. We could see very faint red fluorescence from Fig. 6, and there was negligible difference in cellular red fluorescence for both nanoparticles in COS7 cells, indicating that the RGD modified MSNs selectively target and bind to cancer cells.

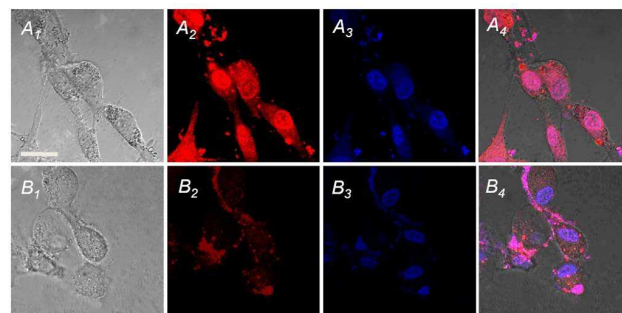


Fig. 5 Confocal laser scanning microscopy (CLSM) images of U-87 MG cells treated by RRMSN/DOX and CRRMSN/DOX for 4 h. A₁₋₄) U-87 MG cells co-incubated with RRMSN/DOX; B₁₋₄) U-87 MG cells co-incubated with CRRMSN/DOX. Image 1: bright field; image 2: red fluorescence field; image 3: blue fluorescence field; image 4: overlapped field. Scale bar: 20 μm.

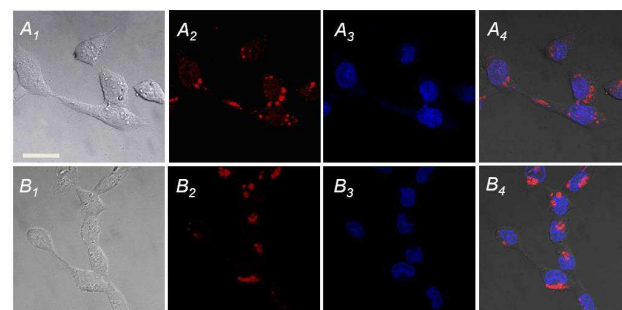


Fig. 6 Confocal laser scanning microscopy (CLSM) images of COS7 cells treated by RRMSN/DOX and CRRMSN/DOX for 4 h. A₁₋₄) COS7 cells co-incubated with RRMSN/DOX; B₁₋₄) COS7 cells co-incubated with CRRMSN/DOX. Image 1: bright field; image 2: red fluorescence field; image 3: blue fluorescence field; image 4: overlapped field. Scale bar: 20 μm .

Cellular Uptake Measured by Flow Cytometry

Flow cytometry analysis was also used to evaluate the cellular uptake behavior of RRMSN/DOX and CRRMSN/DOX in two cell lines quantitatively. As shown in Fig. 7, the U-87 MG cells cellular uptake of RRMSN/DOX was obviously higher than that of CRRMSN/DOX and the mean fluorescence intensity (MFI) value from U-87 MG cells incubating with RRMSN/DOX was 2.4-fold higher than that of CRRMSN/DOX. On the contrary, there was a little difference between the MFI values for COS7 cells. CLSM and flow cytometry results demonstrated that RRMSN/DOX tended to be internalized into U-87 MG cells *via* receptor-mediated endocytosis, which was consistent with the literature report.⁵⁰

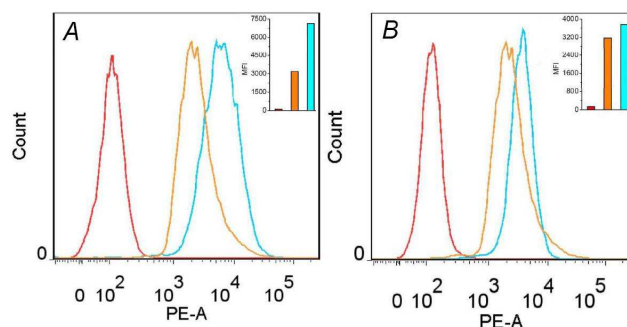


Fig. 7 Flow cytometry analysis of U-87 MG cells (A) and COS7 cells (B) treated with the RRMSN/DOX (green), CRRMSN/DOX (orange) and blank (red) for 4 h. The concentration of DOX was 2.5 $\mu\text{g}/\text{mL}$.

In Vitro Cytotoxicity

As we all know, targeted drug delivery into cancer cells can efficiently enhance the intracellular drug concentration and inhibit the cell growth, and ultimately lead its death. It was found that from Fig. 8, the cell viability of U-87 MG cells was about 7% after co-incubation with RRMSN/DOX for 4 h, while the cell viability of COS7 cells was 40%, at a DOX concentration of 0.5 $\mu\text{g}/\text{mL}$. The more toxicity of U-87 MG cells than that of COS7 cells was due to the enhanced cellular internalization of nanoparticles through RGD-integrin interactions with the aid of RGD moiety. Furthermore, the *in vitro* cytotoxicity of U-87 MG and COS7 cells co-incubated with RRMSN/DOX and CRRMSN/DOX were evaluated. As shown in Fig. 9, the cell viability of U-87 MG cells after co-incubated with RRMSN/DOX for 4 h was approximately 10%, while with regard to the CRRMSN/DOX, the cell viability was about 50% correspondingly. The reason is also attributed to the RGD receptor-mediated endocytosis. However, nearly no difference could be found in COS7 cells between the two types of RRMSN/DOX and CRRMSN/DOX nanoparticles because of absence of targeting effect. As exhibited in Fig. S10, there was a little discrepancy in cell viability between U-87 MG cells and COS7 cells, co-incubated with RRMSN, and the toxicity in U-87 MG cells was a little bit higher due to the enhanced cellular

internalization of nanoparticles with existence of RGD target.

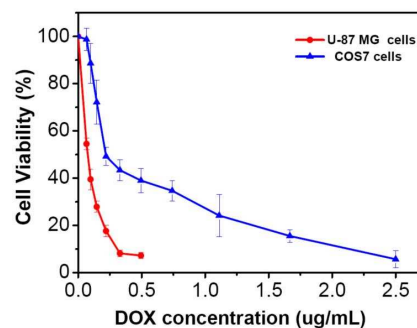


Fig. 8 Viability of U-87 MG cells and COS7 cells after co-incubated with RRMSN/DOX. The concentration of DOX was 2.5 $\mu\text{g}/\text{mL}$.

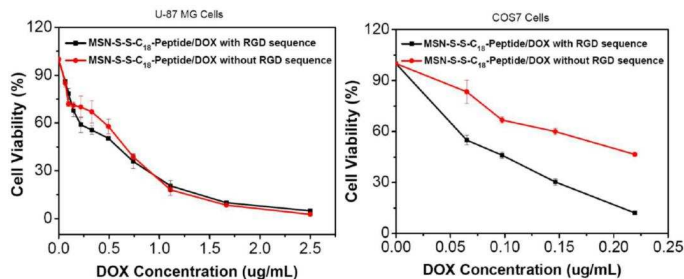


Fig. 9 Viability of U-87 MG cells and COS7 cells after co-incubated with RRMSN/DOX and CRRMSN/DOX. The concentration of DOX was 2.5 $\mu\text{g}/\text{mL}$.

Conclusions

In summary, a redox-responsive mesoporous silica nanoparticle (RRMSN/DOX) was constructed as a drug nanocarrier with amphiphilic peptide based gatekeeper. *In vitro* drug release profiles demonstrated that DOX could be entrapped with nearly no leakage in absence of DTT or GSH, realizing “zero release”. *In vitro* cell research proved that after internalization of MSNs by cancer cells *via* the receptor-mediated endocytosis, the surface amphiphilic peptides and alkyl chains of RRMSN/DOX would be removed to induce rapid drug release intracellularly after the cleavage of disulfide bond inside cancer cells. This novel RRMSN/DOX drug delivery system developed by self-assembly of amphiphilic peptides onto MSNs would provide a facile, but effective strategy for the development of smart and targeted drug carriers for cancer therapy.

Acknowledgements

This work was supported by the National Natural Science Foundation of China (51125014, 51233003 and 21474077), the Ministry of Science and Technology of China (2011CB606202), the Natural Science Foundation of Hubei Province of China (2013CFA003) and the Fundamental Research Funds for the Central Universities.

Notes and references

Key Laboratory of Biomedical Polymers of Ministry of Education & Department of Chemistry, Wuhan University, Wuhan 430072, P. R. China. Fax: +86 27 6875 4509; Tel.: +86 27 6875 5993; E-mail: xz zhang@whu.edu.cn (X.Z. Zhang)

† Electronic Supplementary Information (ESI) available: Experimental details, synthesis and characteristic data, and additional spectra and imaging data. See DOI: 10.1039/b000000x/

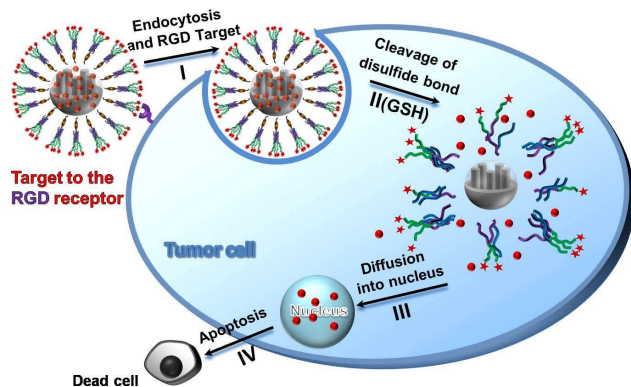
- 1 L. Bldstein, C. Dubernet, P. Couvreur, *Adv. Drug Deliv. Rev.* **2011**, *63*, 3.
- 2 B. P. Timko, T. Dvir, D. S. Kohane, *Adv. Mater.* **2010**, *22*, 4925.
- 3 P. Shi, Z. Liu, K. Dong, E. Ju, J. S. Ren, Y. D. Du, Z. Q. Li, X. G. Qu, *Adv. Mater.* **2014**, *26*, 6635.
- 4 X. M. Li, L. Zhou, Y. Wei, A. M. El-Toni, F. Zhang, D. Y. Zhao, *J. Am. Chem. Soc.* **2014**, *136*, 15086.
- 5 Y. M. Yang, B. Velmurugant, X. G. Liu, B. G. Xing, *Small.* **2013**, *9*, 2937.
- 6 T. M. Guardado-Alvarez, L. S. Devi, M. M. Russell, B. J. Schwartz, J. I. Zink, *J. Am. Chem. Soc.* **2013**, *135*, 14000.
- 7 J. Gallo, N. Kamaly, I. Lavdas, E. Stevens, Q. D. Nguyen, M. Wylezinska-Arridge, E. O. Aboagye, N. J. Long, *Angew. Chem. Int. Ed.* **2014**, *53*, 9500.
- 8 J. Gallo, N. J. Long, E. O. Aboagye, *Chem. Soc. Rev.* **2013**, *42*, 7816.
- 9 Q. J. He, J. L. Shi, *J. Mater. Chem.* **2011**, *21*, 5845.
- 10 J. Zhang, X. D. Xu, Y. Liu, C. W. Liu, X. H. Chen, C. Li, R. X. Zhuo, X. Z. Zhang, *Adv. Funct. Mater.* **2012**, *22*, 1704.
- 11 M. Bouchoucha, R. C. Gaudreault, M. A. Fortin, F. Kleitz, *Adv. Funct. Mater.* **2014**, *24*, 5911.
- 12 Z. Luo, K. Y. Cai, Y. Hu, L. Zhao, P. Liu, L. Duan, W. H. Yang, *Angew. Chem. Int. Ed.* **2011**, *50*, 640.
- 13 J. N. Liu, W. B. Bu, L. M. Pan, J. L. Shi, *Angew. Chem. Int. Ed.* **2013**, *52*, 4375.
- 14 C. Wang, Z. X. Li, D. Cao, Y. L. Zhao, J. W. Gaines, O. A. Bozdemir, M. W. Ambrogio, M. Frascioni, Y. Y. Botros, J. I. Zink, J. F. Stoddart, *Angew. Chem. Int. Ed.* **2012**, *51*, 5460.
- 15 Z. Y. Li, J. J. Hu, Q. Xu, S. Chen, H. Z. Jia, Y. X. Sun, R. X. Zhuo, X. Z. Zhang, *J. Mater. Chem. B.* **2015**, *3*, 39.
- 16 H. Kim, S. Kim, C. Park, H. Lee, H. J. Park, C. Kim, *Adv. Mater.* **2010**, *22*, 4280.
- 17 R. Guillet-Nicolas, A. Popat, J. L. Bridot, G. Monteith, S. Z. Qiao, F. Kleitz, *Angew. Chem. Int. Ed.* **2013**, *52*, 2318.
- 18 Q. Fu, G. V. Rao, T. L. Ward, Y. Lu, G. P. Lopez, *Langmuir.* **2007**, *23*, 170.
- 19 D. P. Ferris, Y. L. Zhao, N. M. Khashab, H. A. Khatib, J. F. Stoddart, J. I. Zink, *J. Am. Chem. Soc.* **2009**, *131*, 1686.
- 20 R. Casasus, M. D. Marcos, R. Martínez-Mañez, J. V. Ros-Lis, J. Soto, L. A. Villaescusa, P. Amorós, D. Beltran, C. Guillem, L. Latorre, *J. Am. Chem. Soc.* **2004**, *126*, 8612.
- 21 A. Popat, B. P. Ross, J. Liu, S. Jambhrunkar, F. Kletiz, S. Z. Qiao, *Angew. Chem. Int. Ed.* **2012**, *51*, 12486.
- 22 C. R. Thomas, D. P. Ferris, J. H. Lee, E. Choi, M. H. Cho, E. S. Kim, J. F. Stoddart, J. S. Shin, J. Cheon, J. I. Zink, *J. Am. Chem. Soc.* **2010**, *132*, 10623.
- 23 Z. Y. Zhou, D. Zhang, S. M. Zhu, *J. Mater. Chem.* **2007**, *17*, 2418.
- 24 C. Park, K. Lee, C. Kim, *Angew. Chem. Int. Ed.* **2009**, *48*, 1275.
- 25 C. Coll, L. Mondragon, R. Martínez-Mañez, F. Sancenón, M. D. Marcos, J. Soto, P. Amorós, E. Perez-Paya, *Angew. Chem. Int. Ed.* **2011**, *50*, 2138.
- 26 P. D. Thornton, A. Heise, *J. Am. Chem. Soc.* **2010**, *132*, 2024.
- 27 Z. Y. Zhou, D. Zhang, S. M. Zhu, *J. Mater. Chem.* **2007**, *17*, 2418.
- 28 F. Muhammad, M. Guo, W. X. Qi, F. X. Sun, A. F. Wang, Y. J. Guo, G. S. Zhu, *J. Am. Chem. Soc.* **2011**, *133*, 8778.
- 29 C. H. Lee, S. H. Cheng, I. P. Huang, J. S. Souris, C. S. Yang, C. Y. Mou, L. W. Lo, *Angew. Chem. Int. Ed.* **2010**, *122*, 8390.
- 30 J. Zhang, Z. F. Yuan, Y. Wang, W. H. Chen, G. F. Luo, S. X. Cheng, R. X. Zhuo, X. Z. Zhang, *J. Am. Chem. Soc.* **2013**, *135*, 5068.
- 31 X. Q. Yang, J. J. Grailer, S. Pilla, D. A. Steeber, S. Q. Gong, *Bioconjugate Chem.* **2010**, *21*, 496.
- 32 W. Wang, R. T. Borchard, B. Wang, *Curr. Med. Chem.* **2000**, *7*, 437.
- 33 V. P. Torchilin, *Adv. Drug Deliv. Rev.* **2008**, *60*, 548.
- 34 M. M. J. Kamphuis, A. P. R. Johnston, G. K. Such, H. H. Dam, R. A. Evans, A. M. Scott, E. C. Nice, J. K. Heath, F. Cruso, *J. Am. Chem. Soc.* **2010**, *132*, 15881.
- 35 J. D. Hood, D. A. Cheresch, *Nat. Rev. Cancer.* **2002**, *2*, 91.
- 36 S. L. Hart, R. P. Harbottle, R. Cooper, A. Miller, R. Williamson, C. Coutelle, *Gene Ther.* **1995**, *2*, 552.
- 37 R. Liu, X. Zhao, T. Wu, P. Y. Feng, *J. Am. Chem. Soc.* **2008**, *130*, 14418.
- 38 G. B. Fields, R. L. Noble, *Int. J. Pept. Protein Res.* **1990**, *35*, 161.
- 39 S. H. Cheng, C. H. Lee, M. C. Chen, J. S. Souris, F. G. Tseng, C. S. Yang, C. Y. Mou, C. T. Chen, L. W. Lo, *J. Mater. Chem.* **2010**, *20*, 6149.
- 40 D. P. Ferris, J. Lu, C. Gothard, R. Yanes, C. R. Thomas, J. C. Olsen, J. F. Stoddart, F. Tamanoi, J. I. Zink, *Small.* **2011**, *7*, 1816.
- 41 S. Lin, N. Chen, S. Sun, J. Chang, Y. Wang, C. Yang, L. Lo, *J. Am. Chem. Soc.* **2010**, *132*, 8309.
- 42 J. Fuente, C. C. Berry, *Bioconjugate Chem.* **2005**, *16*, 1176.
- 43 C. Y. Quan, J. X. Chen, H. Y. Wang, C. Li, C. Chang, X. Z. Zhang, R. X. Zhuo, *ACS Nano.* **2010**, *4*, 4211.
- 44 A. Qin, J. W. Lam, B. Z. Tang, *Chem. Soc. Rev.* **2010**, *39*, 2522.
- 45 R. Liu, X. Zhao, T. Wu, P. Y. Feng, *J. Am. Chem. Soc.* **2008**, *130*, 14418.
- 46 R. Liu, Y. Zhang, P. Y. Feng, *J. Am. Chem. Soc.* **2009**, *131*, 15128.
- 47 G. B. Fields, R. L. Noble, *Int. J. Pept. Protein Res.* **1990**, *35*, 161.
- 48 D. R. Radu, C. Y. Lai, K. Jeftinija, E. W. Rowe, S. Jeftinija, V. S. Lin, *J. Am. Chem. Soc.* **2004**, *126*, 13216.
- 49 Z. H. Zhao, D. T. Huang, Z. Y. Yin, X. M. Wang, J. H. Gao, *J. Mater. Chem.* **2012**, *22*, 15717.
- 50 J. X. Gu, W. P. Cheng, J. G. Liu, S. Y. Lo, D. Smith, X. Z. Qu, Z. Z. Yang, *Biomacromolecules.* **2008**, *9*, 255.
- 51 W. Z. Sun, W. B. Qu, L. Zhao, *J. Chem. Eng. Data.* **2010**, *55*, 4476.
- 52 G. F. Luo, W. H. Chen, Y. Liu, J. Zhang, S. X. Cheng, R. X. Zhuo, X. Z. Zhang, *J. Mater. Chem. B.* **2013**, *1*, 5723.
- 53 C. Y. Lai, B. G. Trewyn, D. M. Jeftinija, K. Jeftinija, S. Xu, S. Jeftinija, S. Y. Lin, *J. Am. Chem. Soc.* **2003**, *125*, 4451.
- 54 R. Hernandez, H. R. Tseng, J. W. Wong, J. F. Stoddart, J. I. Zink, *J. Am. Chem. Soc.* **2004**, *126*, 3370.
- 55 T. D. Nguyen, Y. Liu, S. Saha, K. C. F. Leung, J. F. Stoddart, J. I. Zink, *J. Am. Chem. Soc.* **2007**, *129*, 626.

The table of contents

5 A Redox-Responsive Mesoporous Silica Nanoparticle Capped with Amphiphilic Peptides by Self-assembly for Cancer Targeting Drug Delivery

By Dong Xiao, Hui-Zhen Jia, Ning Ma, Ren-Xi Zhuo, and Xian-Zheng Zhang

10 A novel redox-responsive mesoporous silica nanoparticle (RRMSN/DOX) capped with amphiphilic peptides by self-assembly was demonstrated for targeting drug delivery in cancer cells. After internalization of RRMSN/DOX by cancer cells *via* the receptor-mediated endocytosis, the surface amphiphilic peptides and alkyl chains of RRMSN/DOX would be removed to induce rapid drug release intracellularly after the cleavage of disulfide bond, triggered by GSH secreted in cancer cells.



15